The Weak-Link Approach: Quantum Chemical Studies of the Key Binuclear Synthetic Intermediates

Bradley J. Holliday, Frederick P. Arnold, Jr.,* and Chad A. Mirkin*

Department of Chemistry and Center for Nanofabrication and Molecular Self-Assembly, 2145 Sheridan Road, Northwestern University, Evanston, Illinois 60208-3113

Received: September 12, 2002; In Final Form: February 4, 2003

Gradient-corrected density functional theory calculations have resulted in geometry-optimized structures for a series of six large dirhodium complexes that are important synthetic intermediates in the weak-link synthetic approach. Analysis of these computed structures and their electronic makeup (including natural localized molecular orbital (NLMO) bond order analysis, natural population analysis (NPA) atomic charges, atoms-in-molecules (AIM) calculations, single-point energy analysis, and calculated vibrational frequency analysis) has provided insight into subtle secondary ligand−ligand effects, which lead to product selection in the first step of this synthetic strategy toward supramolecular coordination complexes.

Introduction

The field of supramolecular chemistry continues to be one of prolific growth. As this progress continues, the interest in general, high-yielding synthetic methodologies that facilitate the construction of supramolecular systems with preconceived architectural features remains unabated. The use of transition metal centers and carefully designed ligands has provided a way of synthesizing a wide variety of structures, including metallomacrocycles and other hierarchical structures, which possess unusual chemical and physical properties.[1] One synthetic strategy, the weak-link approach, takes advantage of transition metal centers and bifunctional *hemilabile* ligands[2] to construct large binuclear macrocyclic structures in a two-step and high-yielding process, Scheme 1.[3]

Recent advances in many *organic* synthetic methodologies have been closely coupled to theoretical investigations, and it is this collaborative arrangement that has led to many fundamental changes in how reactivity is considered and new discoveries are made. Although the coupling of synthetic advances and theoretical understanding has been utilized extensively for small organic systems, the analogous study of larger supramolecular structures has lagged behind.[4] The use of theoretical calculations to study metal-driven supramolecular chemistry has been limited because of the prohibitive theoretical expense (calculation time) of such calculations and the absence of methods that can accurately handle transition metal centers.[5] Consequently, reports of detailed theoretical investigations involving transition metal centers have been restricted to relatively small model systems.[6] Herein, we report the density functional theory (DFT) calculations of large (binuclear) metal-containing supramolecular systems and some preliminary insights into the bonding modes and noncovalent forces playing a role in the weak-link approach that are gained through these calculations coupled with experimental investigations.

Theoretical Methods

The calculated structures (**6**−**11**) were optimized on a 16 processor (14 Athlon 800 MHz/1 2-way PIII 933 MHz) cluster running NPACI Rocks (http://rocks.npaci.edu) software, a Linux-based clustering software. The geometric optimizations, single-point calculations, and frequency generations required between 800 and 1200 processor hours per structure.

SCHEME 1

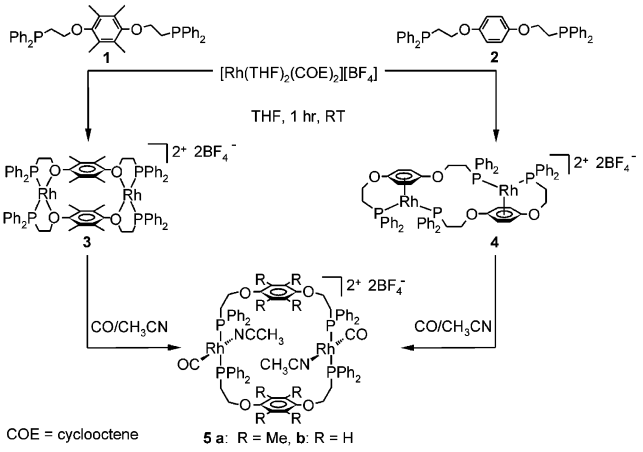

The structural optimizations (in vacuo) were performed using QChem 2.01,[7] 3-21G* basis set, and the EDF1 functional.[8] Structural optimizations were performed within the reported symmetry constraints (C_2 for **6**, **8**, and **10**; C_i for **7** and **9**; and C_1 for **11**). Geometries of **6**−**9** were verified to be local minima by numerical frequency calculations (see Supporting Information). Natural localized molecular orbitals (NLMO)[9] bond order analysis was performed using NBO 4.0m[10] interfaced to GAMESS-US[11] on the basis of single-point energies with the following theoretical model: B3LYP functional, SBKJC ECP and valence basis set, d-polarization functions on all heavy atoms.[12] We have attempted to obtain more accurate energies by using a composite energy, $E_{\text{total}} = E(\text{basis 2}) + D(E(\text{basis 3}) - E(\text{basis 1})) + \text{ZPE(EDF1/3-21G*)}$. The single-point energies were calculated using the GAMESS-US implementation of the B3LYP hybrid functional in spherical variational space with one of the following basis sets. The basis sets are defined as follows: Basis set 1 consists of SBKJC ECP and valence basis set with d-polarization functions on all heavy atoms; basis set 2 consists of SBKJC ECP with 2 d and 1 f

* To whom correspondence should be addressed. Fax: (847) 467-5123. E-mail addresses: fparnold@chem.northwestern.edu or camirkin@chem.northwestern.edu.

10.1021/jp022071l CCC: $25.00
Published on Web 03/25/2003

polarization function on all heavy atoms (standard Pople d-function from basis set 1 with splitting factors of 0.4, 1.4), p polarization on hydrogens, and optimized[13] f polarization on Rh ($\zeta = 0.996\,488$); basis set 3 consists of basis set 1 and diffuse s and p functions on all heavy atoms except Rh. This method is similar to that used by Gordon and co-workers[14] with the exception that our systems are too large for post-Hartree−Fock calculations on computational resources available to us. A test calculation on the first carbonyl dissociation energy from $Ni(CO)_4$ utilizing our methods yielded ΔE of −25.6 kcal/mol and $\Delta H°$ of −23.1 kcal/mol, in good agreement with previous experimental ($\Delta H^{298} = -22$ to −27 kcal/mol) and theoretical ($\Delta E = -23.6$ to −29.8 kcal/mol, $\Delta H° = -22.3$ kcal/mol) work.[15] To make the calculations tractable, the phenyl substituents on the phosphine groups were replaced with methyl groups in structures **6**−**8**. Atoms-in-molecules (AIM) analysis[16] was performed using Morphy 1.0.[17]

Results and Discussion

Our group previously reported the characterization and reactivity of a series of Rh(I)- and Pd(II)-based homobimetallic macrocyclic structures and their corresponding condensed intermediates, prepared via the weak-link approach.[3] We have explored the generality of this synthetic scheme toward different ligand variations including changes in the heteroatom, aromatic spacer, and methylene-linker length. In this body of work, we have observed two distinct isomeric structures that form as condensed intermediates, **3** and **4**, which differ with respect to the ligand-binding modes to the Rh(I) metal centers (Scheme 1). These two complexes have been isolated and thoroughly characterized in solution and by single-crystal X-ray diffraction studies.[3a,c] Under otherwise identical reaction conditions, the reaction of ligand **1** or **2** (Scheme 1) with a reactive Rh(I) precursor results in quantitative yield of either **3** or **4**, respectively. These structures have been descriptively termed the "bow-tie" (**3**) and "slipped" (**4**) structures. It is important to note that either of these intermediate structures can be reacted with coordinating small molecules (e.g., CO and CH_3CN) to form the target macrocycles **5a**,**b** in quantitative yield (Scheme 1). However, it was this variation in binding mode of the condensed intermediate structure with a relatively minor structural change to the ligand that prompted the study reported herein.

This study is aimed at answering four basic questions: (1) Is the theoretical study of these large dirhodium complexes a tractable problem with DFT utilizing a meaningful basis set? (2) If so, can the calculated structures accurately reproduce the different metal−ligand binding modes to give insight into the interactions that drive this assembly process? (3) Can the current theoretical methods be used to determine how ligand substitution affects the distribution of observed intermediates (bow-tie vs slipped); indeed, ligand variation simultaneously affects the basicity of the oxygen atoms, the bulkiness of the arene rings, the binding ability of the arene rings, and the $\pi-\pi$ stacking affinity of the arene rings? (4) Finally, can these theoretical investigations, which neglect solvation and anionic effects,[18] lend meaningful insight into the relative thermodynamic stability of these two isomers?

Comparison of Optimized and X-ray Diffraction Structures. To elucidate the factors controlling the formation of the observed product, either **3** or **4** depending on ligand design, we initiated a computational study of the four possible condensed intermediate structures (slipped and bow-tie isomers of each ligand) resulting from the reaction outlined in Scheme 1. The resulting structures are shown in Figures 1 and 2.

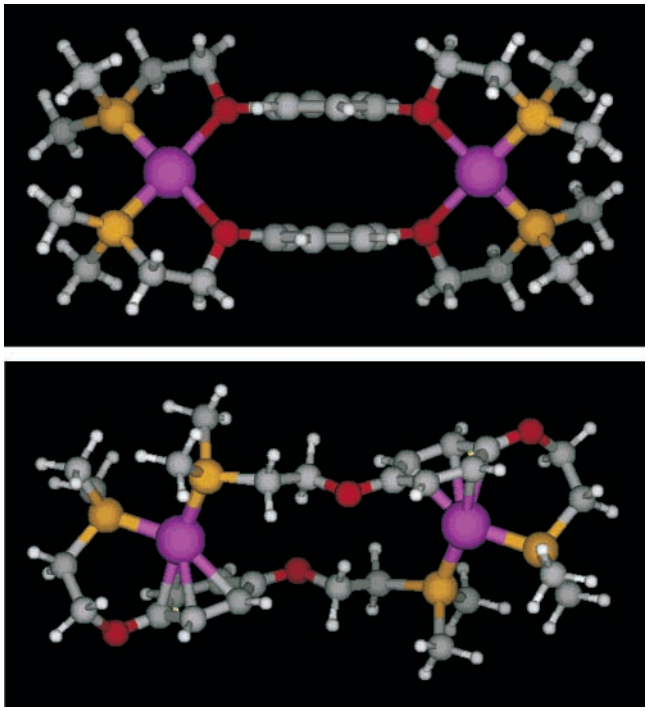

Figure 1. Ball and stick representations of optimized structures of **6** (benzene bow-tie, top) and **7** (benzene slipped, bottom). Colors represent the following: purple, rhodium; yellow, phosphorus; red, oxygen; gray, carbon; white, hydrogen.

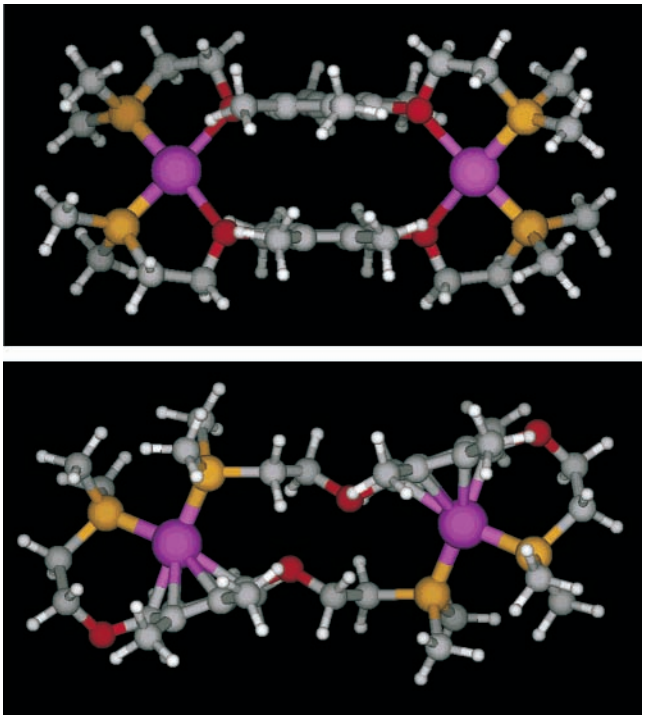

Figure 2. Ball and stick representations of optimized structures of **8** (durene bow-tie, top) and **9** (durene slipped, bottom). Colors represent the following: purple, rhodium; yellow, phosphorus; red, oxygen; gray, carbon; white, hydrogen.

As a gauge of the accuracy of the computed structures **6**−**9**, a detailed comparison between the available X-ray analysis data of the experimentally prepared complexes **3** and **4** and the resulting optimized structures **7** and **8** was performed. The calculated structures were found to be in excellent agreement with the X-ray diffraction data (see Table 1). The mean deviations in the bond lengths of the computed structures from

TABLE 1: Selected Bond Lengths (Å), Bond Angles (deg), Bond Orders, and Atomic Charges of Computed and Solid-State Rhodium Complexes

	X-ray analysis		calculated structures					
entry	**3**	**4**	**6**	**7**	**8**	**9**	**10**	**11**
Rh−O[a]	2.232		2.314		2.334 (0.102)		2.294	
Rh−P_i[b]	2.171	2.295	2.187	2.286 (−0.009)[d]	2.192 (0.021)	2.284	2.195	2.285 (−0.010)
Rh−P_e[b]		2.274		2.247 (−0.027)		2.260		2.246 (−0.028)
P−Rh−P	98.4	95.1	95	95 (−0.1)	94 (−4.4)	94	97	97 (1.9)
O−Rh−O	98.7		102		103 (4.3)		98	
P−Rh−O	81.8		81.8		81.6 (−0.2)		82.1	
Rh−C1		2.444		2.579 (0.135)		2.393		2.612 (0.168)
Rh−C2		2.405		2.563 (0.158)		2.491		2.543 (0.138)
Rh−C3		2.321		2.356 (0.035)		2.416		2.400 (0.079)
Rh−C4		2.276		2.305 (0.029)		2.302		2.299 (0.023)
Rh−C5		2.400		2.394 (−0.006)		2.485		2.374 (−0.026)
Rh−C6		2.316		2.456 (0.140)		2.454		2.533 (0.217)
C_6c-C_6c[c]	3.32		3.623		3.648 (0.33)		3.55	
$\bar{x}_{b.l.}$[e]				0.067	0.061			0.086
$\bar{x}_{b.a.}$[f]					3.0			
				NLMO Bond Orders				
Rh−O			0.07	0.00	0.06	0.00	0.06	0.00
Rh−P_i[b]			0.73	0.65	0.72	0.64	0.69	0.64
Rh−P_e[b]				0.76		0.67		0.75
Rh−C1				0.21		0.25		0.11
Rh−C2				0.19		0.23		0.10
Rh−C3				0.16		0.18		0.14
Rh−C4				0.15		0.15		0.17
Rh−C5				0.12		0.14		0.19
Rh−C6				0.10		0.10		0.14
				NPA Atomic Charges				
Rh			−0.20	−0.22	−0.20	−0.21	−0.18	−0.20
O			−0.66	−0.62	−0.67	−0.64	−0.66	−0.62
P			1.19	1.17	1.18	1.17	1.22	1.20

[a] Average Rh−O bond lengths. [b] Average Rh−P bond length for structures **3**, **6**, **8**, and **10**. For structures **4**, **7**, **9**, and **11**, P_i denotes interior phosphorus atoms and P_e denotes exterior phosphorus atoms. [c] C_6c denotes arene ring centroid. [d] Deviations of calculated values from experimentally determined values are shown in parentheses. [e] Mean of the absolute deviations in the selected bond lengths. [f] Mean of the absolute deviations in the selected bond angles.

the experimental data are less than 0.1 Å for all structures, the largest single deviation being 0.217 Å. Surprisingly, despite the change in substitution on the phosphine moiety, the bond distances, bond angles, and torsional angles around these atoms remain consistent with the observed X-ray data. There are undoubtedly steric and electronic differences between the calculated structures and the experimentally characterized ones, but for these studies, the assumption is that by comparing the two intermediates these differences are minimized. Others have made analogous assumptions when carrying out calculations on large systems.[6a] Finally, to confirm the validity of the calculated model structures (or supply an appropriate correction), the full diphenylphosphine analogues of structures **6** and **7** (bow-tie and slipped), were optimized and single-point calculations were run, structures **10** and **11** in Table 1. These structures compare extremely well with both the dimethylphospine structures (**6** and **7**) and the X-ray data (mean bond length deviation of 0.086 Å, largest deviation 0.217 Å for structure **11**) confirming that the constrained geometry of the condensed intermediates minimizes the effects of phosphorus substitution.

The Rh(I) metal centers display coordination geometries that compare well with the solid-state structures determined by single-crystal X-ray diffraction analysis.[3a,c] Importantly, the interactions of the metal centers with the ligands have been reproduced with a high level of agreement (bond length deviations of ≤0.2 Å). In the benzene slipped structure, **7**, the optimized structure displays an offset transition metal interaction with the arene ring (distorted η^6-binding) that mimics the observed interaction; X-ray data reveal two long (2.405−2.444 Å) Rh−C bonds and four shorter Rh−C bonds (2.276−2.400 Å). The aromatic core groups of each ligand are held in a cofacial, parallel-planar arrangement 3.32 Å apart in the bow-tie structures, complexes **3**, **6**, **8**, and **10**. This distance is well within $\pi-\pi$ stacking distance (3.35 Å for graphite),[19] which requires that the aromatic substituents be interdigitated. This results in an 18° twist between the two aromatic rings of structure **3**. This interaction is accurately reproduced in the calculated complexes (15° twist angle). The twist displayed by the aromatic rings is also consistent with relatively strong van der Waals interactions between the methyl groups in **8**; the groups display an offset alignment presumably to maximize these van der Waals contacts and minimize repulsive steric interactions (vide infra).

Bonding Analysis of Structures 6−9. The atomic charges (Natural Population Analysis (NPA)[20] methods) have been determined at each atom (Table 1) in the calculated complexes. The NPA method reveals that the bow-tie structures (**6** and **8**) have slightly less negative oxygen atoms, and the oxygen atoms of the durene structures (**8** and **9**) are more negative than those of the benzene complexes (**6** and **7**). This indicates an accurate reproduction of the different binding modes in the two isomeric structures observed and that the increased electron density of the durene aromatic core in **1** is moderately delocalized on the adjacent oxygen atoms. NLMO[9] bond order analysis confirms the presence of an extremely weak Rh−O interaction in structures **6** and **8**, which have bond orders of 0.07 and 0.06, respectively. These weak bonding interactions are consistent with the selective displacement of these bonds by incoming ancillary ligands of moderate coordinating ability (i.e., CH_3CN).[3] However, this observation also points to factors other

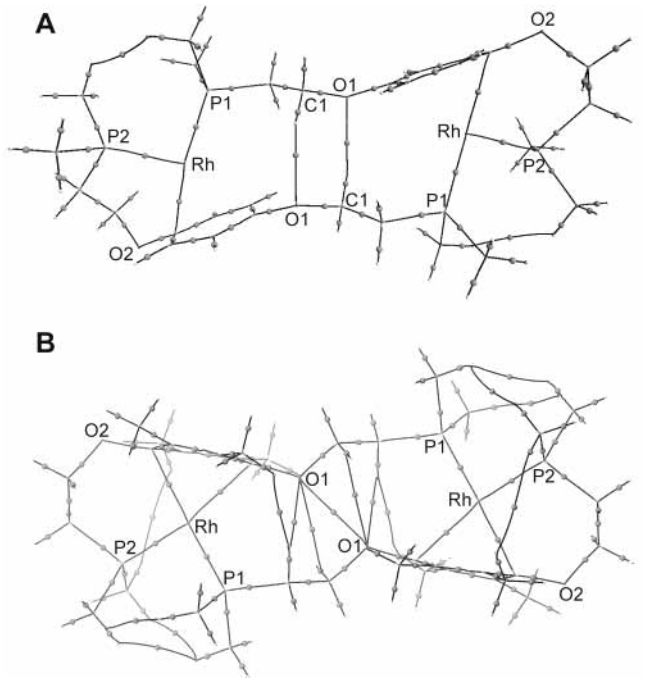

Figure 3. Stylized view of (A) complex **7** showing bond critical points (balls) and bond paths as determined by AIM calculations and (B) complex **9** with depth shading for clarity showing bond critical points (balls) and bond paths as determined by AIM calculations.

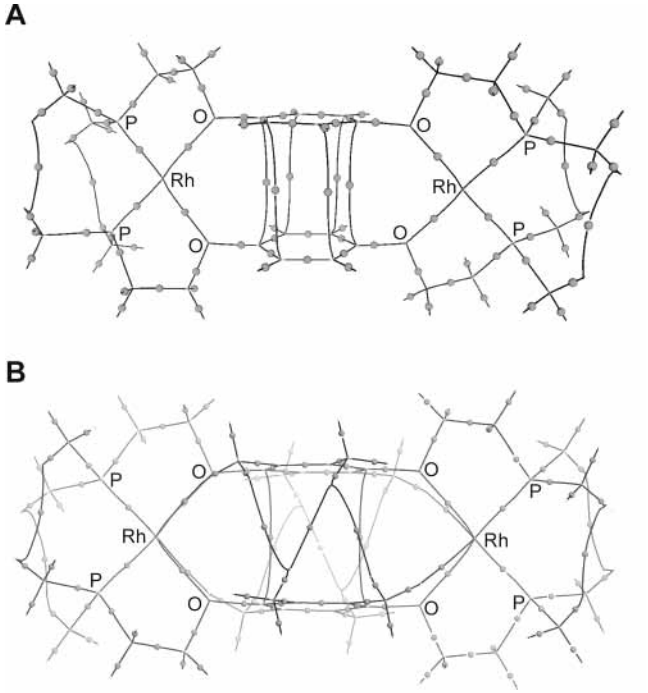

Figure 4. Stylized view of (A) complex **6** showing bond critical points (balls) and bond paths as determined by AIM calculations and (B) complex **8** with depth shading for clarity showing bond critical points (balls) and bond paths as determined by AIM calculations.

than Rh−O bond strength that stabilize the bow-tie durene structure because the aromatic group is clearly a better donor to the metal center.

AIM Calculations in Structures 6−9. To further clarify the situation, AIM calculations[16] using the Huzinaga MIDI basis set[21] augmented with d-polarization functions on the heavy atoms were performed to analyze the topology of the electron density of these systems. Several interesting features become apparent from the AIM results. As shown in Figures 3 and 4, the AIM analysis identifies noncovalent bonding features, which stabilize the slipped and bow-tie structures. In the case of the slipped structures (**7**, Figure 3A; **9**, Figure 3B), the AIM analysis shows strong interactions between the methylene protons on the interior of the slipped structures and the oxygen atoms (O1) opposite them; this interaction is present in both slipped structures. Further, in the durene structure (**9**) there exists a bond critical point and bond path connecting the oxygen atoms as well. On the basis of the relative positions of the bond and ring critical points in the hydrogen bonds versus the O−O bonding interaction, one would expect the O−O interaction to be a more important stabilizing factor in the slipped durene structure. However, the hydrogen bond critical points in this structure are closely associated with ring critical points, which indicates that a small structural distortion will cause the critical points to merge and annihilate one another, thereby breaking the hydrogen bond and destabilizing structure **9**. The arene−metal interaction can also be addressed by this method. In structure **7** (Figure 3A), there is one contact point between each arene ring and the metal center. In contrast, the durene analogue (Figure 3B) has two metal−arene contacts due to the increased donor ability of the electron-rich ring. In the bow-tie structures (Figure 4), several stabilizing features become apparent. There are significant ring−ring contacts (on the order of hydrogen-bonding interactions) in both bow-tie structures, but the nature of the interactions are quite different. In the case of structure **6** (Figure 4A), there are carbon−carbon contacts present at each carbon atom of the central benzene ring. The durene structure, **8** (Figure 4B), displays a somewhat different interaction. First, the only carbons of the rings that display a direct interring interaction are the carbons directly bound to the oxygen atoms. Second, the AIM analysis reveals a web of hydrogen−hydrogen interactions[22] between the methyl groups of the durene rings that stabilize this stacked structure. These contacts account for the twist of the two rings relative to one another (vide supra). Therefore, the AIM calculations provide evidence for the notion that the methyl substituents lead to increased van der Waals and dihydrogen contacts, which stabilize structure **8**. This effect should be enhanced by increasing the aliphatic substituents about the arene ring, provided that the aliphatic substituents do not lead to unfavorable steric interactions in the bow-tie structure. Additionally, the AIM analysis provides information about the coordination bonds. As one would expect empirically, there is

TABLE 2: Energetics (hartrees) of Calculated Structures

entry	**6**	**7**	**8**	**9**	**10**	**11**
basis set 1	−495.953 466	−495.943 886	−550.590 083	−550.579 891	−730.702 351	−730.690 574
basis set 2	−496.189 423	−496.172 223	−550.866 423	−550.849 398		
basis set 3	−496.008 664	−495.984 807	−550.659 431	−550.632 822		
ZPE correction	0.717 506	0.715 569	0.945 412	0.935 711		
basis set 2 − basis set 1	−0.235 957	−0.228 336	−0.276 340	−0.269 506		
basis set 3 − basis set 1	−0.055 198	−0.040 920	−0.069 348	−0.052 931		
energy total	−495.527 120	−495.497 580	−549.990 359	−549.966 617		

a weak but significant Rh−O interaction of the same magnitude as the Rh−arene interactions. The values for ρ at the Rh−O bond critical points are 0.065 and 0.066 e/au^3 (structures **6** and **8**, respectively), confirming the presence of a slightly stronger Rh−O bond in the durene system, thereby stabilizing the bow-tie geometry.

Relative Energetics of Structures 6−9. The energies of the calculated structures have been determined at the corresponding local minima (Table 2). The calculations indicate the lowest energy structure for each ligand set to be the bow-tie structure. While a comparison of complexes comprised of different ligands is invalid (e.g., **6** and **8**), the consideration of energy differences in the two sets of complexes with similar ligand environments (e.g., **6** and **7**, **8** and **9**) provides insight into the theoretically predicted relative thermodynamic stability of the intermediate structures. In the case of the benzene-based ligand, complexes **6** and **7**, it was determined that the energy difference between the two structures was 18.5 kcal/mol in favor of the bow-tie structure, **6**. Similarly, the durene-based complexes (**8** and **9**) display an energy difference of 15.5 kcal/mol, with the lower energy structure also being the bow-tie, **8**. This discrepancy with the experimentally observed species in the case of the benzene-based ligand system is likely a result of the assumptions made in these calculations that neglect the role of solvent and anions in this system. Both have been shown to affect the reaction experimentally.[3c,h] However, on the basis of the accurate $Ni(CO)_4$ dissociation energy test calculation (see methods section), we can be confident in the *gas-phase* energies reported here.

The information gained from the calculations on these systems (vide supra) indicates that the oxygen atoms in these hemilabile ligands bind weakly to Rh(I) in this ligand environment and that the observed product distributions are heavily influenced by the $\pi-\pi$ and van der Waals interactions of the central aromatic groups. However, this Rh−O bonding can be enhanced by increasing the electron density of the oxygen atoms by substituting the central ring with electron-donating groups. Analysis of isodesmic reactions (eqs 1 and 2) to quantitatively

$$\text{benzene slipped complex } (\mathbf{7}) + 4C_2H_6 \rightarrow \text{durene slipped complex } (\mathbf{9}) + 4H_2 + 47.2 \text{ kcal/mol} \quad (1)$$

$$\text{benzene bow-tie complex } (\mathbf{6}) + 4C_2H_6 \rightarrow \text{durene bow-tie complex } (\mathbf{8}) + 4H_2 + 50.8 \text{ kcal/mol} \quad (2)$$

determine the effect of methylation of the core arene reveals that the slipped structure is less destabilized by removing the methyl groups, but the bow-tie structure is moderately more stable with the durene group present, which we attribute to the additional contacts displayed in the AIM structures (vide supra, Figures 3 and 4).

Conclusions

In conclusion, this study reports the detailed DFT calculations of six large homobinuclear Rh(I) complexes assembled with hemilabile ligands. These structures are direct analogues of important synthetic intermediates in the weak-link approach to supramolecular coordination compounds, and analysis of the calculated complexes lends insight into subtle ligand−ligand interactions and uncommon bonding motifs that cumulatively stabilize the coordination isomers studied. However, the calculations reported herein, which neglect the important effects of solvation and ion pairing to be manageable, fall short of accurately describing the energetic aspects of product distribution in this reaction. The predicted energy differences are relatively small and solvation or anion effects could readily account for this discrepancy. Nevertheless, this study is important because it identifies that secondary ligand−ligand interactions (arene−arene interactions), as well as the direct metal−ligand interactions, stabilize the intermediate structures in the weak-link synthetic approach.

Acknowledgment. C.A.M. and F.P.A. acknowledge NSF (Grant CHE-9628768), NSF/MRSEC (Grant DMR-0076097), and Georgia Institute of Technology Molecular Design Institute (ONR Contract No. N-00014-95-1-1116) for support of this research. B.J.H. acknowledges Sigma Xi and the Link Foundation for fellowship support.

Supporting Information Available: Tables of atomic coordinates and computed frequencies of structures **6**−**9**. Tables of atomic coordinates of structures **10** and **11**. Additional orientations of **6**−**9** and **10** and **11** (32 pages). This material is available free of charge via the Internet at http://pubs.acs.org.

References and Notes

(1) (a) Holliday, B. J.; Mirkin, C. A. *Angew. Chem., Int. Ed.* **2001**, *40*, 2022−2043. (b) Leininger, S.; Olenyuk, B.; Stang, P. J. *Chem. Rev.* **2000**, *100*, 853−908. (c) Caulder, D. L.; Raymond, K. N. *J. Chem. Soc., Dalton Trans.* **1999**, 1185−1200. (d) Swiegers, G. F.; Malefetse, T. J. *Chem. Rev.* **2000**, *100*, 3483−3537. (e) Fujita, M.; Umemoto, K.; Yoshizawa, M.; Fujita, N.; Kusukawa, T.; Biradha, K. *Chem. Commun.* **2001**, 509−518.

(2) (a) Bader, A.; Lindner, E. *Coord. Chem. Rev.* **1991**, *108*, 27−110. (b) Slone, C. S.; Weinberger, D. A.; Mirkin, C. A. In *Progress In Inorganic Chemistry*; Karlin, K. D., Ed.; Wiley: New York, 1999; Vol. 48, pp 233−350.

(3) (a) Farrell, J. R.; Mirkin, C. A.; Guzei, I. A.; Liable-Sands, L. M.; Rheingold, A. L. *Angew. Chem., Int. Ed.* **1998**, *37*, 465−467. (b) Farrell, J. R.; Mirkin, C. A.; Liable-Sands, L. M.; Rheingold, A. L. *J. Am. Chem. Soc.* **1998**, *120*, 11834−11835. (c) Farrell, J. R.; Eisenberg, A. H.; Mirkin, C. A.; Guzei, I. A.; Liable-Sands, L. M.; Incarvito, C. D.; Rheingold, A. L.; Stern, C. L. *Organometallics* **1999**, *18*, 4856−4868. (d) Holliday, B. J.; Farrell, J. R.; Mirkin, C. A.; Lam, K.-C.; Rheingold, A. L. *J. Am. Chem. Soc.* **1999**, *121*, 6316−6317. (e) Dixon, F. M.; Eisenberg, A. H.; Farrell, J. R.; Mirkin, C. A.; Liable-Sands, L. M.; Rheingold, A. L. *Inorg. Chem.* **2000**, *39*, 3432−3433. (f) Eisenberg, A. H.; Dixon, F. M.; Mirkin, C. A.; Stern, C. L.; Incarvito, C. D.; Rheingold, A. L. *Organometallics* **2001**, *20*, 2052−2058. (g) Liu, X.; Eisenberg, A. H.; Mirkin, C. A.; Stern, C. L. *Inorg. Chem.* **2001**, *40*, 2940−2941. (h) Liu, X.; Stern, C. L.; Mirkin, C. A. *Organometallics* **2002**, *21*, 1017−1019. (i) Ovchinnikov, M. V.; Holliday, B. J.; Mirkin, C. A.; Zakharov, L. N.; Rheingold, A. L. *Proc. Natl. Acad. Sci. U.S.A.* **2002**, *99*, 4927−4931. (j) Holliday, B. J.; Jeon, Y.-M.; Mirkin, C. A.; Stern, C. L.; Incarvito, C. D.; Zakharov, L. N.; Sommer, R. D.; Rheingold, A. L. *Organometallics* **2002**, *21*, 5713−5725.

(4) Some notable exceptions: (a) Tse, J. S. In *Comprehensive Supramolecular Chemistry*; Atwood, J. L., et al., Eds.; Elsevier: Oxford, U.K., 1996; pp 593−616. (b) Castro, R.; Berardi, M. J.; Córdova, E.; Ochoa de Olza, M.; Kaifer, A. E.; Evanseck, J. D. *J. Am. Chem. Soc.* **1996**, *118*, 10257−10268. (c) Rauwolf, C.; Strassner, T. *J. Mol. Model.* **1997**, *3*, 1−16. (d) Sharma, S.; Radhakrishnan, T. P. *J. Phys. Chem. B* **2000**, *104*, 10191−10195. (e) Rana, D.; Gangopadhyay, G. *Chem. Phys. Lett.* **2001**, *334*, 314−324. (f) Ochsenfeld, C.; Brown, S. P.; Schnell, I.; Gauss, J.; Spiess, H. W. *J. Am. Chem. Soc.* **2001**, *123*, 2597−2606. (g) Brown, S. P.; Schaller, T.; Seelbach, U. P.; Koziol, F.; Ochsenfeld, C.; Klarner, G.; Spiess, H. W. *Angew. Chem., Int. Ed.* **2001**, *40*, 717−720.

(5) Puchta, R.; Seitz, V.; van Eikema Hommes, N. J. R.; Saalfrank, R. W. *J. Mol. Model.* **2000**, *6*, 126−132.

(6) Some representative examples: (a) Gherman, B. F.; Dunietz, B. D.; Whittington, D. A.; Lippard, S. J.; Friesner, R. A. *J. Am. Chem. Soc.* **2001**, *123*, 3836−3837. (b) Andruniow, T.; Zgierski, M. Z.; Kozlowski, P. M. *J. Am. Chem. Soc.* **2001**, *123*, 2679−2680. (c) Webster, C. E.; Hall, M. B. *J. Am. Chem. Soc.* **2001**, *123*, 5820−5821. (d) de Bruin, T. J. M.; Milet, A.; Robert, F.; Gimbert, Y.; Greene, A. E. *J. Am. Chem. Soc.* **2001**, *123*, 7184−7185. (e) Wondimagegn, T.; Ghosh, A. *J. Am. Chem. Soc.* **2001**, *123*, 1543−1544. (f) Seminario, J. M.; De La Cruz, C. E.; Derosa, P. A. *J. Am. Chem. Soc.* **2001**, *123*, 5616−5617. (g) Dunietz, B. D.; Beachy, M. D.; Cao, Y.; Whittington, D. A.; Lippard, S. J.; Friesner, R. A. *J. Am. Chem. Soc.* **2000**, *122*, 2828−2839.

(7) Q-Chem 2.0: A high-performance ab initio electronic structure program. Kong, J.; White, C. A.; Krylov, A. I.; Sherrill, C. D.; Adamson, R. D.; Furlani, T. R.; Lee, M. S.; Lee, A. M.; Gwaltney, S. R.; Adams, T. R.; Ochsenfeld, C.; Gilbert, A. T. B.; Kedziora, G. S.; Rassolov, V. A.; Maurice, D. R.; Nair, N.; Shao, Y.; Besley, N. A.; Maslen, P. E.; Dombroski, J. P.; Daschel, H.; Zhang, W.; Korambath, P. P.; Baker, J.; Byrd, E. F. C.; Van Voorhis, T.; Oumi, M.; Hirata, S.; Hsu, C.-P.; Ishikawa, N.; Florian, J.; Warshel, A.; Johnson, B. G.; Gill, P. M. W.; Head-Gordon, M.; Pople, J. A. *J. Comput. Chem.* **2000**, *21*, 1532−1548.

(8) Adamson, R. D.; Gill, P. M. W.; Pople, J. A. *Chem. Phys. Lett.* **1998**, *284*, 6−11.

(9) Reed, A. E.; Weinhold, F. *J. Chem. Phys.* **1985**, *83*, 1736−1740.

(10) Glendening, E. D.; Badenhoop, J. K.; Reed, A. E.; Carpenter, J. E.; Weinhold, F. *NBO 4.0M*; Theoretical Chemistry Institute, University of Wisconsin: Madison, WI, 1999.

(11) Schmidt, M. W.; Baldridge, K. K.; Boatz, J. A.; Elbert, S. T.; Gordon, M. S.; Jensen, J. H.; Koseki, S.; Matsunaga, N.; Nguyen, K. A.; Su, S. J.; Windus, T. L.; Dupuis, M.; Montgomery, J. A. *J. Comput. Chem.* **1993**, *14*, 1347−1363.

(12) (a) Stevens, W. J.; Basch, H.; Krauss, M. *J. Chem. Phys.* **1984**, *81*, 6026−6033. (b) Stevens, W. J.; Krauss, M.; Basch, H.; Jasien, P. G. *Can. J. Chem.* **1992**, *70*, 612−630. (c) Cundari, T. R.; Stevens, W. J. *J. Chem. Phys.* **1993**, *98*, 5555−5565.

(13) Optimized for Rh(0) ^{4}F state, MP2 trudge optimization in GAMESS-US.

(14) Merrill, G. N.; Gordon, M. S. *J. Chem. Phys.* **1999**, *110*, 6154−6157.

(15) Ehlers, A. W.; Frenking, G. *Organometallics* **1995**, *14*, 423−426 and references therein.

(16) Bader, R. F. W. *Atoms in Molecules, a Quantum Theory*; Oxford Press: Oxford, U.K., 1990.

(17) Popelier, P. L. A. *Comput. Phys. Commun.* **1996**, *93*, 212−240.

(18) (a) Liu, X.; Stern, C. L.; Mirkin, C. A. *Organometallics* **2002**, *21*, 1017−1019. (b) Schweiger, M.; Seidel, S. R.; Arif, A. M.; Stang, P. J. *Inorg. Chem.* **2002**, *41*, 2556−2559. (c) Campos-Fernandez, C. S.; Clerac, R.; Koomen, J. M.; Russell, D. H.; Dunbar, K. R. *J. Am. Chem. Soc.* **2001**, *123*, 773−774.

(19) Shriver, D. F.; Atkins, P.; Langford, C. H. *Inorganic Chemistry*, 2nd. ed.; W. H. Freeman: New York, 1997.

(20) (a) Reed, A. E.; Weinhold, F. *J. Chem. Phys.* **1983**, *78*, 4066−4073. (b) Reed, A. E.; Weinstock, R. B.; Weinhold, F. *J. Chem. Phys.* **1985**, *83*, 735−746.

(21) *Gaussian Basis Sets for Molecular Calculations*; Huzinaga, S., Ed.; Elsevier: Amsterdam, 1984.

(22) (a) Richardson, T. B.; de Gala, S.; Crabtree, R. H.; Siegbahn, P. E. M. *J. Am. Chem. Soc.* **1995**, *117*, 12875−12876. (b) Arnold, F. P. *J. Organomet. Chem.* **2001**, *617*−*618*, 647−655.